Progress In Electromagnetics Research, PIER 81, 237–252, 2008

ANALYSIS OF WAVE FUNCTION, ENERGY AND TRANSMISSION COEFFICIENTS IN GAN/ALGAN SUPERLATTICE NANOSTRUCTURES

K. Talele and D. S. Patil

Department of Electronics
North Maharashtra University
Jalgaon, Maharashtra, India

Abstract—Analysis of wave function intensity, eigen energy and transmission coefficients in GaN/AlGaN superlattice nanostructure has been carried out using Transfer Matrix Method (TMM). The effect of change in Aluminum mole fraction in $Al_xGa_{1-x}N$ barrier region has been included through variable effective mass in the Schrödinger time independent equation. The behaviour of wave function intensity has been studied for superlattice structure by changing the barrier width. The effect of smaller barrier width on wave function intensity in case of superlattice is clearly observed due to interaction of wave functions in the adjacent wells and it provides a new insight in the nature of interacting wave functions for thin barriers in GaN/AlGaN superlattice structures. The barrier widths have been optimized for the varying number of wells leading to better quantum confinement. The iterative method (Secant Method) is used to determine value of electron energy E. The number of iterations need to converge the value of E has been simulated. Transmission coefficients have been determined as a function of energy E considering tunneling effect for three well structures using TMM. Analysis has been extended to show surface image of wave function intensity for 5 and 6 wells.

1. INTRODUCTION

Intensive research work has been carried out for the development of efficient optoelectronics devices based on quantum nanostructures. Recently, wide band gap III-V nitride semiconductor materials [1, 2] have received much attention due to their high potential for applications in optoelectronic devices, which covers wide range of spectrum from green-to-ultraviolet spectral region. These nitrides

provide potential for the expansion of semiconductor technology for various applications ranging from televisions, traffic signals, scanners, flashlights, high-density optical storage memories and automotive backlighting [3, 4]. The promising features of the devices made from nitride materials provide long lifetime and proved to be superior to ZnSe and its alloys in optoelectronic applications [5, 6]. However, ZnSe has low thermal conductivity, poor thermal stability and large ohmic contact resistances. The recent developments in the field of GaN-based light emitting devices have stimulated several experimental and theoretical studies on GaN/AlGaN heterostructures [7].

Advances in material growth technologies particularly molecular beam epitaxy [8] and metal-organic chemical vapor deposition [9] make the fabrication of high quality quantum nanostructures possible. In a quantum well structure, a series of energy levels and associated sub bands are formed due to quantization of carriers in the direction of quantum well thickness. The carrier confinement and its resulting density of states in quantum wells promise more efficient lasing devices. When the quantum wells of Gallium Nitride are sandwich between the $Al_xGa_{1-x}N$ barriers, it provides an excellent electron confinement.

Semiconductor lasers benefit from the use of multiple quantum wells (MQW) and superlattice [10–12] nanostructures. The advantages of using such complex structures are high modal differential gain, reduced threshold current and higher characteristics temperature. The carrier wave functions obtained through the solutions to the Schrödinger equation [13–15] in the periodic potential of the lattice is localized in space and the corresponding energy eigen values are discrete. The effect of the periodic potential of the crystal lattice on the electrons is treated by introducing an effective electron mass.

Despite of the large number of reports on the fabrication and optical characterization of nitride-based devices, there have been a small number of theoretical investigations of electronic wave function intensities and transport mechanism in complex nanostructures. The advantages and opportunities associated with quantum nanostructures are escorted by challenges. Perhaps of greatest concern are the superlattice structures with many wells separated by relatively thin barrier layers. The coupling between electronic states localized in semiconductor nanostructures is a matter of great interest for both fundamental and device oriented reasons. It is well known that, when the attenuation length of the electronic wave function into the barriers becomes comparable with the barrier thickness, the carrier tunneling between adjacent quantum wells modifies significantly the recombination kinetics and transport properties. The proper account of these phenomena provides a new insight in the nature of overlapping

the wave functions for thin barriers in GaN/AlGaN superlattice nanostructures having both fundamental and applied relevance. However, in spite of the extensive applications of GaN/AlGaN nanostructures for light emitting diodes and efficient short wavelength visible and ultraviolet lasers, theoretical understanding is still not complete.

Therefore, main objective of the paper is to study behavior of wave functions in the wells and their overlapping with adjacent wells if thickness of AlGaN barrier region is reduced. The barrier widths have been optimized for the better quantum confinement for the varying number of wells. In this paper, we present investigation of wave function intensities along with their surface images and effect of barrier thickness in superlattice nanostructures. The wave function intensity has been calculated by squaring wave function amplitude for the varying number of wells from 3 to 7. Transfer matrix method (TMM) [16] is a simple and accurate numerical method that can be used for a wide range of problems dealing with second-order differential equations. Therefore, TMM has been used to obtain solutions of Schrodinger equation in well and barrier regions. The simulation is carried out using MATLAB software. Transmission coefficients have been determined for superlattice structures with varying Aluminum mole fraction. Furthermore, we deduced the bound state energy as a function of variation in effective mass of electron in the barrier and barrier height with aluminum concentration for both the nanostructures. The computational efforts needed to compute energy through secant method has been simulated in terms of number of iterations.

The paper is organized as follows. In Section 2, we present the theoretical analysis of solving Schrodinger equation using TMM. Section 3 illustrates results of wave function intensities along with surface images for varying number of wells. Furthermore, results of transmission coefficients and energy have been discussed for superlattice structures of GaN/$Al_xGa_{1-x}N$ [17–19]. Finally, conclusions are summarized.

2. THEORETICAL ANALYSIS

Recently, there has been a considerable increase in research interest directed towards the development of optoelectronic devices based on quantum well heterostructures [20–23], guided wave devices [24–26] and quantum nanostructures [27, 28]. To understand the physical properties of device structures, it is important to simulate the expected performance on a computer. Here, we use transfer matrix method for

its simplicity and to provide a reasonable accuracy. We have considered the variation of the effective mass and barrier height of AlGaN barrier with aluminum concentration into the calculations. The fundamental equation that describes the electron spatial behavior by determining wave function $\psi(x)$, is the time independent Schrodinger equation. The standard Schrodinger equation can be written for each of the quantum nanostructure layers is as follows:

$$\partial^2\psi(x)/\partial x^2 + (8m^*\pi^2/h^2)(E-V)\psi(x)=0 \quad \text{in the AlGaN barrier} \tag{1}$$

$$\partial^2\psi(x)/\partial x^2 + (8m^*\pi^2/h^2)E\psi(x)=0 \quad \text{in the GaN well} \tag{2}$$

At this juncture, E is the energy of electron, conduction band potential is zero and effective mass of electron m^* equal to m_w in the well region and in the barrier region conduction band potential is V and m^* is m_b.

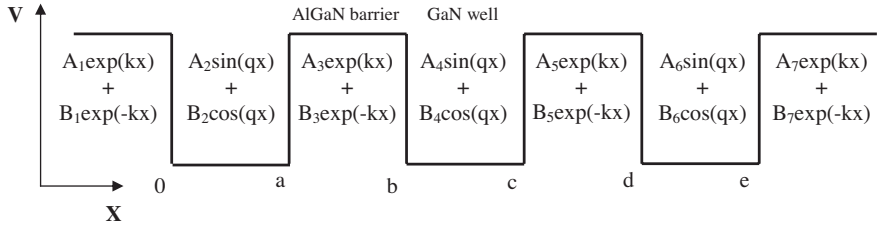

Figure 1. Quantum nanostructure consisting of 3 wells with solutions.

For the proper confinement of the electrons in the well, the energy E must be less than barrier height V. The superlattice nanostructures considered for the theoretical analysis for 3 wells is as shown in Fig. 1. The general solutions of the Schrodinger equation for this quantum nanostructure are as follows:

$$\begin{aligned}
\psi(x) &= A_1\exp(kx) + B_1\exp(-kx), \quad x<0\\
\psi(x) &= A_2\sin(qx) + B_2\cos(qx), \quad 0<x<a\\
\psi(x) &= A_3\exp(kx) + B_3\exp(-kx), \quad a<x<b\\
\psi(x) &= A_4\sin(qx) + A_4\cos(qx), \quad b<x<c\\
\psi(x) &= A_5\exp(kx) + A_5\exp(-kx), \quad c<x<d\\
\psi(x) &= A_6\sin(qx) + B_6\cos(qx), \quad d<x<e\\
\psi(x) &= A_7\exp(kx) + B_7\exp(-kx), \quad x>e
\end{aligned} \tag{3}$$

where, $q^2 = (8m^*\pi^2/h^2)E$ and $k^2 = (8m^*\pi^2/h^2)(V-E)$.

The q and k are the wave vectors in quantum well and barrier region. These, wave vectors are determined by substituting value of E

that has been obtained through an iterative method (secant method). Considering continuity of wave function and its first derivative at the each interface of well and barrier region for 3 well structure as follows: At $x = 0$,

$$\begin{aligned} A_1 + B_1 &= B_2 \\ 1/m_b(kA_1) - kB_1) &= 1/m_w(qA_2) \end{aligned} \tag{4}$$

At $x = a$,

$$\begin{aligned} A_2\sin(qa) + B_2\cos(qa) &= A_3\exp(ka) + B_3\exp(-ka) \\ 1/m_w[qA_2\cos(qa) - qB_2\sin(qa)] &= 1/m_b[kA_3\exp(ka) - kB_3\exp(-ka)] \end{aligned} \tag{5}$$

At $x = b$,

$$\begin{aligned} A_3\exp(kb) + B_3\exp(-kb) &= A_4\sin(qb) + B_4\cos(qb) \\ 1/m_b[kA_3\exp(kb) - kB_3\exp(-kb)] &= 1/m_w[qA_4\cos(qb) - qB_4\sin(qb)] \end{aligned} \tag{6}$$

At $x = c$:

$$\begin{aligned} A_4\sin(qc) + B_4\cos(qc) &= A_5\exp(kc) + B_5\exp(-kc) \\ 1/m_w[qA_4\cos(qc) - qB_4\sin(qc)] &= 1/m_b[kA_5\exp(kc) - kB_5\exp(-kc)] \end{aligned} \tag{7}$$

At $x = d$:

$$\begin{aligned} A_5\exp(kd) + B_5\exp(-kd) &= A_6\sin(qd) + B_6\cos(qd) \\ 1/m_b[kA_5\exp(kd) - kB_5\exp(-kd)] &= 1/m_w[qA_6\cos(qd) + qB_6\sin(qd)] \end{aligned} \tag{8}$$

At $x = e$:

$$\begin{aligned} A_6\sin(qe) + B_6\cos(qe) &= A_7\exp(ke) + B_7\exp(-ke) \\ 1/m_w[qA_6\cos(qe) - qB_6\sin(qe)] &= 1/m_b[kA_7\exp(ke) - kB_7\exp(-ke) \end{aligned} \tag{9}$$

In matrix form these equations are written as

$$\begin{aligned} &\begin{bmatrix} 1 & 1 \\ \dfrac{k}{m_b} & \dfrac{-k}{m_b} \end{bmatrix} \begin{bmatrix} A_1 \\ B_1 \end{bmatrix} = \begin{bmatrix} 0 & 1 \\ \dfrac{q}{m_w} & 0 \end{bmatrix} \begin{bmatrix} A_2 \\ B_2 \end{bmatrix} \\ &\begin{bmatrix} \sin(qa) & \cos(qa) \\ (q/m_w)\cos(qa) & (-q/m_w)\sin(qa) \end{bmatrix} \begin{bmatrix} A_2 \\ B_2 \end{bmatrix} \\ &= \begin{bmatrix} \exp(ka) & \exp(-ka) \\ (k/m_b)\exp(ka) & (-k/m_b)\exp(ka) \end{bmatrix} \begin{bmatrix} A_3 \\ B_3 \end{bmatrix} \\ &\begin{bmatrix} \exp(kb) & \exp(-kb) \\ (k/m_b)\exp(kb) & (-k/m_b)\exp(-kb) \end{bmatrix} \begin{bmatrix} A_3 \\ B_3 \end{bmatrix} \\ &= \begin{bmatrix} \sin(qb) & \cos(qb) \\ (q/m_w)\cos(qb) & (-q/m_w)\sin(qb) \end{bmatrix} \begin{bmatrix} A_4 \\ B_4 \end{bmatrix} \end{aligned}$$

$$\begin{aligned}
&\begin{bmatrix} \sin(qc) & \cos(qc) \\ (q/m_w)\cos(qc) & (-q/m_w)\sin(qc) \end{bmatrix} \begin{bmatrix} A_4 \\ B_4 \end{bmatrix} \\
&= \begin{bmatrix} \exp(kc) & \exp(-kc) \\ (k/m_b)\exp(kc) & (-k/m_b)\exp(kc) \end{bmatrix} \begin{bmatrix} A_5 \\ B_5 \end{bmatrix} \\
&\begin{bmatrix} \exp(kd) & \exp(-kd) \\ (k/m_b)\exp(kd) & (-k/m_b)\exp(-kd) \end{bmatrix} \begin{bmatrix} A_5 \\ B_5 \end{bmatrix} \\
&= \begin{bmatrix} \sin(qd) & \cos(qd) \\ (q/m_w)\cos(qd) & (-q/m_w)\sin(qd) \end{bmatrix} \begin{bmatrix} A_6 \\ B_6 \end{bmatrix} \\
&\begin{bmatrix} \sin(qe) & \cos(qe) \\ (q/m_w)\cos(qe) & (-q/m_w)\sin(qe) \end{bmatrix} \begin{bmatrix} A_6 \\ B_6 \end{bmatrix} \\
&= \begin{bmatrix} \exp(ke) & \exp(-ke) \\ (k/m_b)\exp(ke) & (-k/m_b)\exp(ke) \end{bmatrix} \begin{bmatrix} A_7 \\ B_7 \end{bmatrix}
\end{aligned} \tag{10}$$

In concise form, equations become

$$M_1 \begin{bmatrix} A_1 \\ B_1 \end{bmatrix} = M_2 \begin{bmatrix} A_2 \\ B_2 \end{bmatrix} \tag{11}$$

$$M_3 \begin{bmatrix} A_2 \\ B_2 \end{bmatrix} = M_4 \begin{bmatrix} A_3 \\ B_3 \end{bmatrix} \tag{12}$$

Rearranging these equations gives,

$$\begin{aligned}
\begin{bmatrix} A_1 \\ B_1 \end{bmatrix} &= M_1^{-1} M_2 \begin{bmatrix} A_2 \\ B_2 \end{bmatrix} \\
\begin{bmatrix} A_2 \\ B_2 \end{bmatrix} &= M_3^{-1} M_4 \begin{bmatrix} A_3 \\ B_3 \end{bmatrix} \\
\begin{bmatrix} A_1 \\ B_1 \end{bmatrix} &= M_1^{-1} M_2 M_3^{-1} M_4 \begin{bmatrix} A_3 \\ B_3 \end{bmatrix}
\end{aligned} \tag{13}$$

Finally, after simplification we get,

$$\begin{bmatrix} A_1 \\ B_1 \end{bmatrix} = M_1^{-1} M_2 M_3^{-1} M_4 M_5^{-1} M_6 M_7^{-1} M_8 M_9^{-1} M_{10} M_{11}^{-1} M_{12} \begin{bmatrix} A_7 \\ B_7 \end{bmatrix} \tag{14}$$

Equation (14) can be written as

$$\begin{bmatrix} A_1 \\ B_1 \end{bmatrix} = M \begin{bmatrix} A_7 \\ B_7 \end{bmatrix} \tag{15}$$

Here,

$$\begin{aligned}
A_1 &= M_{11} A_7 + M_{12} B_7 \\
B_1 &= M_{21} A_7 + M_{22} B_7
\end{aligned} \tag{16}$$

Applying normalization conditions determines unknown coefficients A_n and B_n in above equations to know the exact solution of wave functions. The probability interpretation of the wave function implies that the wave function must tend towards zero at the outer barriers means the coefficients of the growing exponentials must be zero. In this case, with the origin at the 1st interface implies that $B_1 = 0$ and for last interface $A_7 = 0$, and hence above equation would imply that $M_{22} = 0$. As all of the elements of M are function of k and q, which are both in turn function of the energy E, therefore energy satisfies the following condition:

$$M_{22}(E) = 0$$

Once the energy is known through the iterative solutions of wave vectors using secant method, the coefficients A_1 to B_7 follow simply and the envelope wave function has been deduced. Multiplying matrices together for the whole potential profile, the wave functions, and confined energies are found for the whole system. For systems where the states are not bound and properly confined, TMM can be used to calculate the transmission coefficients as

$$T(E) = \frac{1}{M_{11}^* M_{11}} \tag{17}$$

At this point, M_{11} describes first matrix element, which is taken from matrix M and M_{11}^* describes conjugate form of M_{11}.

The motive behind using the transfer matrix method is to obtain the electron energy accurately and to analyze the transmission coefficients concurrently. The transmission coefficient is necessary to study the tunneling of the electron through the quantum well. The transmission coefficient has been an important quantity since it provides most of the relevant information of the transport process in superlattice and it is characterized by a series of resonance peaks at specific incidence energies.

3. RESULTS AND DISCUSSION

We have carried out detail analysis of superlattice nanostructures in which thickness of well region and barrier is of the order of nanometers. The variation of electron energy with effective mass of electron in the barrier region has been studied for superlattice structure as shown in Fig. 2. The values of well width and barrier width are optimized to be 2 nm and 6 nm respectively. The value of Energy E was found to be decreasing with the increase in barrier mass. As the molar

concentration of aluminum increases the barrier mass is increased. We have considered barrier height of 0.3112 eV for both the superlattice consisting of 3 wells. The effective mass of the electron in GaN well region is taken to be $0.2m_0$. With the variation of effective mass of electron in barrier from 0.228 to 0.48, energy was found to be decreasing from 0.2 eV to 0.1624 eV. The decrease in the energy value is due to inverse relation between energy and effective mass.

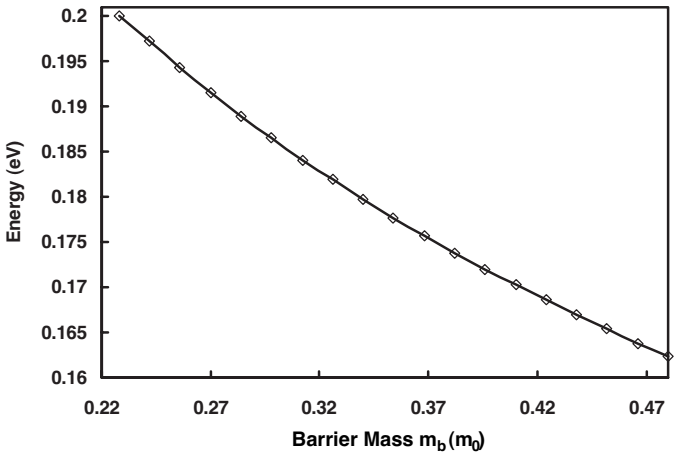

Figure 2. Variation of energy with barrier mass.

Figure 3 depicts dependence of energy on the barrier height and number of iterations needed to converge energy value considering effective mass of electron in the barrier region and well region $0.256m_0$ and $0.2m_0$ respectively. It reveals that value of energy E is increasing with corresponding increase in barrier height due to increase of Aluminum mole fraction in AlGaN barrier. Value of the energy E was found to be increase from 0.0987 to 0.4435 eV with corresponding increase in barrier height from 0.1503 to 1.98 eV. The number of iterations needed to compute value of the electron energy E using iterative method (secant method) for varying values of Aluminum mole fraction x in the barrier explores that with the increasing value of energy E, number of iterations needed to converge are greater in number. The number of iterations needed varies from 3 to 24 with corresponding energy value of 0.1 to 0.445 eV.

The variation in energy with number of wells is shown in Fig. 4. As number of wells is increased from 2 to 8, the energy was found to be decreasing from 0.3 to 0.16 eV. Fig. 5(a) demonstrates the wave function intensity for the 3 wells for three different values of energies 0.1177 eV, 0.1725 eV and 0.2252 eV, which corresponds to

aluminum mole fraction of 0.1, 0.15 and 0.2 respectively. The wave function intensity was computed by squaring the amplitude of the wave function. The electrons are confining in well region because energy is less than the conduction band potential. The solution of Schrodinger equation consist of growing and decaying terms due to which wave function intensity increase in well region and decreases in barrier region. Due to interaction of wave functions between adjacent well regions in super lattice, wave functions overlap with each other. Therefore, wave function intensity in each well never reaches to zero.

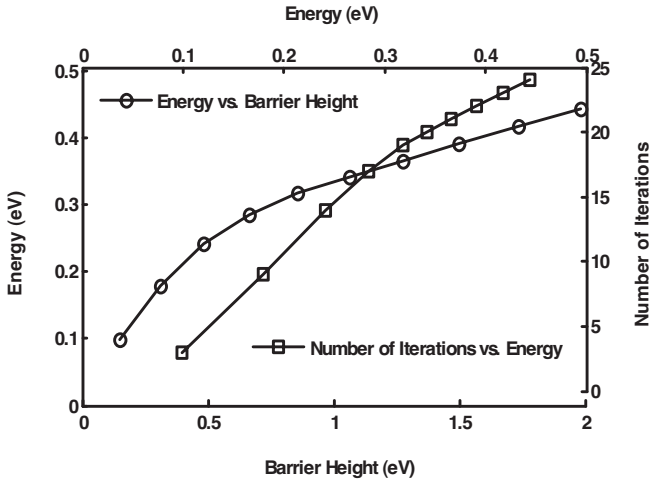

Figure 3. Dependence of energy on barrier height and number of iterations.

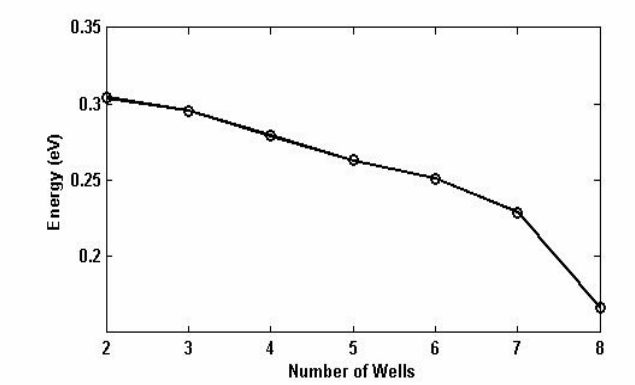

Figure 4. Energy as a function of number of wells.

In three well structures, the wave function intensity is dominant in central well for better confinement in middle of the whole structure than other well regions. Fig. 5(b) shows 3D view of wave function intensity.

Figure 6(a) and Fig. 6(b) exemplifies the wave function intensity and its surface image in the superlattice structure for the even 4 and odd 5 number of wells respectively. The images reveal that the bright bands of almost equal intensities are observed in the two center wells for even number of wells. These bright bands correspond to peak intensities of center two peaks. Corresponding to magnitude of the

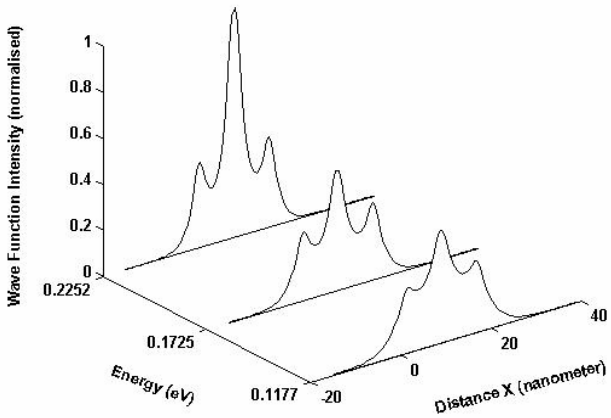

(a)

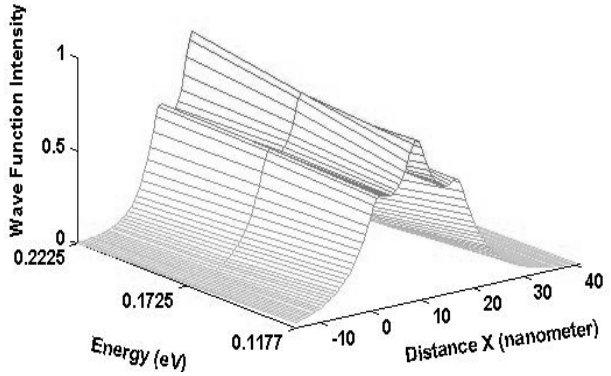

(b)

Figure 5. (a) Wave function intensity in 3 well superlattice structure, (b) 3D view of wave function intensity.

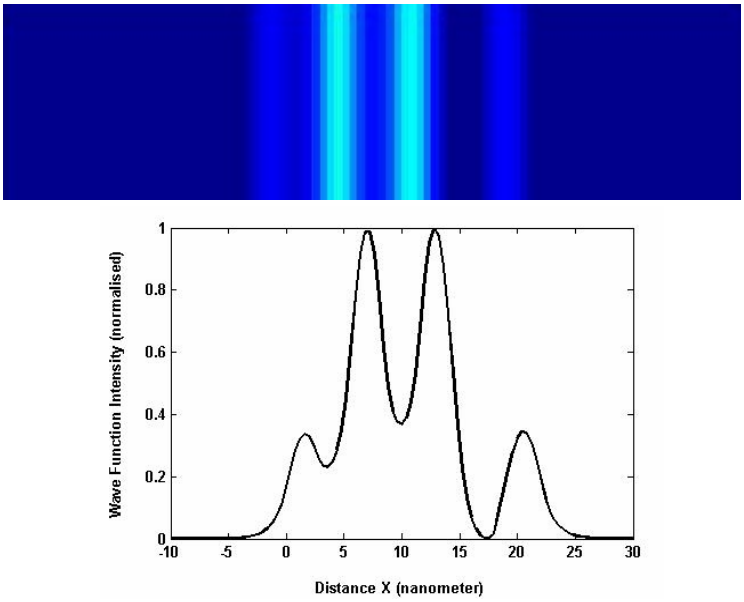

(a)

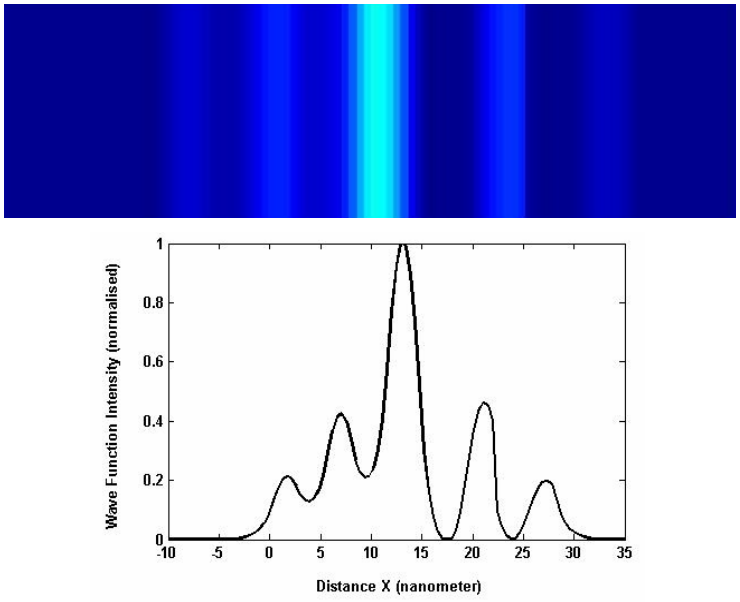

(b)

Figure 6. (a) Wave function intensity and its surface image in 4 well structure, (b) Wave function intensity and its surface image in 5 well structure.

intensities, there is change in the brightness of the bands in the surface image. One bright band has been observed in Fig. 6(b) corresponding to mighty peak of wave function intensity in the central well. For the 4 well structure barrier height of 0.4827 eV and energy of 0.279 eV has been deduced. The energy value of 0.2629 eV has been deduced for the 5 well structures for the same barrier height. The brightness goes on decreasing towards extreme ends of the superlattice due to fall in the peak intensity on the extreme ends. Depending on value of the wave function intensity, there is change in the brightness of the bands. It is found from Fig. 6(a) that the wave function intensities of the inner two wells are identical when the even numbers of wells are present in superlattice structure while for the odd number of wells the center well has the maximum electron confinement as shown in Fig. 6(b).

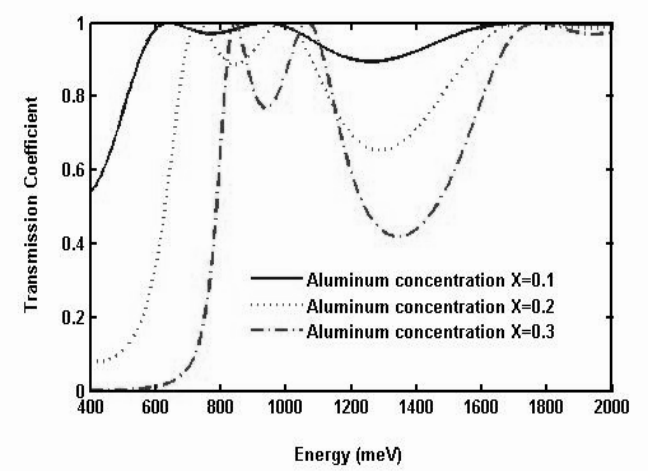

Figure 7. Transmission coefficients as a function of energy.

Figure 7 shows the dependence of transmission coefficient on the energy for different values of Aluminum mole fractions. One way of quantifying the proportion of electrons that tunnel through is in terms of transmission coefficient, which is defined as the probability that any single electron impinging on a barrier structure will tunnel and contribute to the current flow through the barrier. The transmission coefficient becomes complex as energy increases. The wave function decays exponentially if $E < V$ and transmission increases to unity in the barrier region. Transmission coefficient has been deduced for the 3 well superlattice structure. The barrier heights of 0.1503 eV, 0.3112 eV and 0.4827 eV have been estimated corresponding to Aluminum mole fractions of 0.1, 0.2 and 0.3 in the AlGaN barrier. For higher values of

energy, transmission coefficient becomes oscillatory and showed three oscillations corresponding to 3 wells. Transmission coefficient was found to be changing from 0.5383 to 0.9970 for $x = 0.1$, from 0.0823 to 0.9887 for $x = 0.2$ and from 0 to 0.9734 for $x = 0.3$.

4. CONCLUSIONS

Theoretical analysis of wave function intensity, energy and transmission coefficients in superlattice structure has been carried out using TMM and the iterative method has been used to compute value of the energy E. The effect of Aluminum mole fraction in the barrier region has been taken in to account to consider variable effective mass approximation and barrier height. The reduction of thickness of barrier and well region in the superlattice structure has been simulated to the study the change in behavior of the wave function intensity and interaction of wave function in the adjacent wells. The wave function intensity has been deduced along with its surface image and 3D image for the varying even and odd number of wells. Transmission coefficient has been deduced considering tunneling effect. The computational efforts needed to compute value of E through iterative method has been determined. In conclusion, our analysis is very useful to study the performance of complex quantum and superlattice structures exploring its applicability to determine quantum confinement in multi-layer nanostructures.

REFERENCES

1. Yonenaga, I., "High-temperature strength of IIICV nitride crystals," *J. Phys.: Condens. Matter*, Vol. 14, 12947–12951, 2002.
2. Mohammad, S. N., A. A. Salvador, and M. Hadis, "Emerging gallium nitride based devices," *Proceedings of the IEEE*, Vol. 83, No. 10, 1306–1355, 1995.
3. Krishnan, M. S., N. Goldsman, and A. Christou, "Transport simulation of bulk AlxGa1 — xN and the two-dimensional electron gas at the AlxGa1-xN/GaN," *Journal of Applied Physics*, Vol. 83, Issue 11, 5896, 1998.
4. Franssen, G., P. Perlin, and T. Suski, "Photocurrent spectroscopy as a tool for determining piezoelectric fields in InxGa1-xN/GaN multiple quantum well light emitting diodes," *Physical Review B*, Vol. 69, Issue 4, 045310–045316, 2004.
5. Patil, D. S. and D. K. Gautam, "Analysis of effect of temperature

on ZnSSe based blue laser diode characteristics at 507 nm wavelength," *Physica B*, Vol. 344, 140–146, 2004.

6. Patil, D. S. and D. K. Gautam, "Computer analysis and optimization of physical and material parameters of the blue laser diode," *Optics Communications*, Vol. 201, 413–423, 2002.
7. Samuel, E. P., M. P. Bhole, and D. S. Patil, "Mode confinement and near field intensity analysis in a GaN-based blue-green laser diode," *Semiconductor Science and Technology*, Vol. 21, 993–997, 2006.
8. Craven, M. D., P. Waltereit, J. S. Speck, and S. P. Den Baars, "Well-width dependence of photoluminescence emission from a-plane GaNAlGaN multiple quantum wells," *Applied Physics Letters*, Vol. 84, 496, 2004.
9. Christiansen, K., M. Luenenbuerger, B. Schineller, M. Heuken, and H. Juergensen, "Advances in MOCVD technology for research, development and mass production of compound semiconductor devices," *Opto-electronics Review*, Vol. 10, No. 4, 237–242, 2002.
10. Ambacher, O., "Growth and applications of Group III-nitrides," *Journal of Physics D: Applied Physics*, Vol. 31, 2653–2710, 1998.
11. Polyakov, A. Y., N. B. Smirnov, A. V. Govorkov, A. V. Osinsky, P. E. Norris, S. J. Pearton, J. Van Hove, A. M. Wowchack, and P. P. Chow, "Optical properties of undoped n-AlGaN/GaN superlattices as affected by built-in and external-electric field and by Ar-implantation-induced partial disordering," *Journal of Applied Physics*, Vol. 90, 4032, 2001.
12. Abdi-Ben, N. S., N. Sfina, N. Bouarissa, and M. Said, "Modelling of ZnSxSe1-xZnSySe1-y band offsets and QW for green-yellow applications," *Journal of Physics: Condensed Matter*, Vol. 18, 3005–3016, 2006.
13. Ren, Z., R. Venugopal, S. Goasguen, S. Datta, and M. S. Lundstrom, "NanoMOS 2.5: A two-dimensional simulator for quantum transport in double-gate MOSFETs," *IEEE Transactions on Electron Devices*, Vol. 50, No. 9, 1914–1925, 2003.
14. Glanemann, M., V. M. Axt, and T. Kuhn, "Transport of a wave packet through nanostructures: Quantum kinetics of carrier capture processes," *Physical Review B*, Vol. 72, 045354–045366, 2005.
15. Lindblad, H. and A. Soffer, "Scattering and small data completeness for the critical. nonlinear Schrodinger equation," *Nonlinearity*, Vol. 19, 345–353, 2006.

16. Jonsson, B. and T. E. Sverre, "Solving the Schrodinger equation in arbitrary quantum-wellpotential profiles using the transfer matrix method," *IEEE J. Quantum Elecrron*, Vol. 26, No. 11, 2025–2035, 1990.
17. Talele, K., E. P. Samuel, and D. S. Patil, "Investigation of near field intensity in GaN MQW in 300–375 nanometer wavelength ranges," *Journal of Electromagnetic Waves and Applications*, Vol. 22, 1122–1130, 2008.
18. Chen, C.-N., K.-F. Yarn, W.-J. Luo, J.-C. Chiang, I. Lo, W.-T. Wang, M.-H. Gau, H.-F. Kao, M.-E. Lee, W.-C. Chuang, W.-C. Chang, and T.-C. Cheng, "Effects of giant optical anisotropy in R-plane GaN/AlGaN quantum wells by valence band mixing," *PIERS Online*, Vol. 2, No. 6, 562–566, 2006.
19. Garc, A., V. Grimalsky, A. Silva, P. Rivera, A. Morales, and F. Marroqu, "Amplifcation of acoustic-electromagnetic waves in GaN films," *PIERS Online*, Vol. 3, No. 8, 1232–1235, 2007.
20. Chen, C. N., W. C. Chien, K. F. Yarn, S.-H. Chang, and M. Hung, "Intrinsic optical anisotropy in zinc-blende semiconductor quantum wells," *Progress In Electromagnetics Research Letters*, Vol. 22, No. 26, 223–226, 2005.
21. Gaggero-Sager, L. M., N. Moreno-Martinez, I. Rodriguez-Vargas, R. Perez-Alvarez, V. V. Grimalsky, and M. E. Mora-Ramos, "Electronic structure as a function of temperature for Si doped quantum wells in GaAs," *PIERS Online*, Vol. 3, No. 6, 851–854, 2007.
22. Ahmed, I. and A. R. Baghai-Wadji, "1D canonical and perturbed quantum potentialwell problem: A universal function approach," *PIERS Online*, Vol. 3, No. 4, 481–485, 2007.
23. Srivastava, R., S. Pati, and S. P. Ojha, "Enhancement of omnidirectional reflection in photonic crystal heterostructures," *Progress In Electromagnetics Research B*, Vol. 1, 197–208, 2008.
24. Lu, J., B.-I. Wu, J. A. Kong, and M. Chen, "Guided modes with a linearly varying transverse field inside a left-handed dielectric slab," *Journal of Electromagnetic Waves and Applications*, Vol. 20, No. 5, 689–697, 2006.
25. Fan, G. F., J. P. Ning, L. J. Shang, Q. Han, and Z. Q. Chen, "Theoretical analysis and design of non-collinear guided-wave acousto-optic devices," *Journal of Electromagnetic Waves and Applications*, Vol. 20, No. 13, 1837–1844, 2006.

26. Mora-Ramos, M. E., R. Perez-Alvarez, and V. R. Velasco, "The electrostatic potential associated to interface phonon modes in nitride single heterostructures," *Progress In Electromagnetics Research Letters*, Vol. 1, 27–33, 2008.
27. Samuel, E. P. and D. S. Patil, "Analysis of wavefunction distribution in quantum well biased laser diode using transfer matrix method," *Progress In Electromagnetics Research Letters*, Vol. 1, 119–128, 2008.
28. Tarkhanyan, R. H. and N. K. Uzunoglu, "Propagation of electromagnetic waves on the lateral surface of a ferrite/semiconductor superlattice at quantum Hall-effect conditions," *Progress In Electromagnetics Research*, Vol. 29, 321–335, 2000.